Three-wave coupling of microwaves in metamaterial with nonlinear resonant conductive elements

M. Lapine* and M. Gorkunov†
Department of Physics, University of Osnabrück, 49069 Osnabrück, Germany
(Received 1 July 2004; published 1 December 2004)

We consider a metamaterial possessing nonlinear magnetic response owing to nonlinear electronic components inserted into resonant conductive elements. We imply that the insertions operate in an essentially nonlinear regime, so that a nonlinear magnetic susceptibility cannot be introduced and separate analysis is required for different nonlinear processes. Here we develop an approach for analyzing three-wave coupling processes with a strong pump wave and two weak signals. We discuss the peculiarities of coupling arising from use of insertions with variable resistance or variable capacitance. We estimate that extremely strong nonlinear coupling can be achieved using typical diodes reported in the literature.

DOI: 10.1103/PhysRevE.70.066601 PACS number(s): 41.20.Jb, 42.65.Ky, 75.50.−y, 78.20.Bh

I. INTRODUCTION

In the course of several recent years metamaterials have been attracting vast scientific attention. Initial interest in this subject was driven by the idea of realizing negative refraction. Although predicted theoretically by Veselago [1] as early as in 1967, negative refraction remained an abstract idea, as it requires the permittivity and permeability both to be negative, which is nonexistent in natural materials. These requirements can be met in metamaterials—artificial structures, arranged as regular lattice of identical elements or sets of elements. The scale of these structures shifts the working range of metamaterials from optical frequencies to microwaves, but the general description of their electromagnetic response is the same as for crystals. The design of metamaterials was discussed [2] and experiments were reported to be successful [3,4]. At the same time, general electromagnetic properties of the backward waves in Veselago media received a recent review [5].

Obviously, the range of metamaterial applications is not confined to the demonstration and use of the negative refraction phenomenon. Rapid development of microwave technology suggests elaboration of methods for effective and immediate manipulation with microwaves, and metamaterials seem to be especially suitable for this purpose, being a kind of crystal for microwaves. An important advantage is that the metamaterial properties can be adjusted by choosing the structure elements and their arrangement.

If the wavelength of the electromagnetic wave inside the medium is much larger than both the element size and the distances between neighboring elements, the properties of the metastructure with respect to such waves can be described with the macroscopic permittivity and permeability. The typical size of a metamaterial's "atom" (of the order of millimeters) satisfies this requirement for microwaves up to the gigahertz range. Earlier we presented a macroscopic description of a metamaterial organized as a three-dimensional lattice of resonant conductive elements (RCEs) [6,7]. The approach described there has much in common with the classical theory of the optical properties of condensed matter [8–10].

In view of the close analogy to crystals, metamaterials are likely to host direct microwave interaction, provided that the response of the structure elements is nonlinear. The general idea of assembling a nonlinear artificial medium by introducing a nonlinear component within the structure elements has been known since the early 1990s [11], when metamaterials had not yet emerged. Later, active electronic inclusions were suggested for enhancement of the negative band in linear metamaterials [12]. In 2003 two proposals appeared introducing a magnetically nonlinear metamaterial [7,13], and since then this concept has attracted increasing attention [14,15].

In particular, we considered diode insertions into RCEs and discussed the possibility of three-wave coupling in corresponding metamaterials [7]. We have shown that for the case of small amplitudes of the interacting waves, when the diodes are driven by relatively low voltage, the nonlinear response of the metamaterial is described by a quadratic magnetic susceptibility, which can be explicitly expressed via the parameters of structure elements and lattice constants. Accordingly, the magnetization of the medium is given by

$$\mathbf{M}(\omega_2) = \hat{\chi}_{\mathrm{M}}(\omega_2)\mathbf{H}(\omega_2) + \hat{\chi}^{(2)}_{\mathrm{M}}(\omega_2;\omega_0,\omega_1)\mathbf{H}(\omega_0)\mathbf{H}(\omega_1), \tag{1}$$

where $\omega_0+\omega_1=\omega_2$. This provides a general phenomenology for various nonlinear processes analogous to those known in optics, and already for weak amplitudes we estimated the nonlinear modulation to be several orders of magnitude higher than in crystals. However, dissipation losses are also remarkable in such media, and the corresponding imaginary part of the magnetic susceptibility appears to be of the same order as the nonlinear modulation, limiting the range of possible applications.

In search for better characteristics we consider below higher amplitudes of the interacting waves, when an essentially nonlinear range of the insertion characteristic is involved. Under this condition, a universal description (1) of

*Email address: mlapine@uos.de
†Permanent address: Institute of Crystallography RAS, Leninski prospekt 59, 117333 Moscow, Russia.

 ©2004 The American Physical Society

the nonlinear properties of the metamaterial is no longer possible. We have to analyze separately different nonlinear processes and to distinguish between various types of nonlinear insertions.

In this paper we concentrate on the three-wave coupling for a particular class of processes when only one of the waves is a strong pump wave, while the other two are weak signal waves. Among these are parametric amplification, frequency conversion, parametric instability, etc. We analyze the coupling strength arising with use of nonlinear insertions possessing variable resistance and variable capacitance.

II. NONLINEAR COUPLING WITH INSERTIONS AT HIGH NONLINEARITY

Considering nonlinear coupling in a metamaterial, we are interested in the relationship between the magnetization of the metamaterial and the macroscopic magnetic fields inside it, at all the frequencies involved. The magnetization is determined by the currents induced in RCEs by the fields of propagating waves. Should the response of the RCE be nonlinear, a coupling between these currents arises. Consequently, in a metamaterial of RCEs with nonlinear insertions, wave coupling is provided on the level of the structure elements. Thus we are first looking for the relationship between the currents induced at the interacting frequencies, by analyzing a single element, subjected to an oscillating magnetic field.

As in our previous work, we are concerned with arbitrary flat RCEs. If the dimensions of the RCE are smaller than the wavelength, then the element can be described by a linear contour with effective resistance R_c, self-inductance L_c, and capacitance C_c. These parameters can be either estimated theoretically [6] or evaluated experimentally [16]. Note that such consideration is appropriate for complex elements like a split ring resonator [2,16,17], as such an element can be represented by an effective contour, provided that the width of the stripes is small enough compared to the element size [18,19]. Accordingly, the linear properties of the element are described by the impedance $Z(\omega)=R_c-i\omega L_c+i(\omega C_c)^{-1}$, so that a harmonic emf with amplitude $\mathcal{E}$, magnetically induced at frequency ω, drives a harmonic current with amplitude I in accordance with $\mathcal{E}=Z(\omega)I$.

Now we take into account the nonlinear insertions, connected in series to the linear contour. When the insertions operate in the highly nonlinear regime, the resulting time dependencies of voltages and currents in general do not have to be harmonic. In order to deal with harmonic interacting waves in a metamaterial, we assume that the contribution of insertions to the response of the structure element is small. Under this assumption, we neglect inharmonicity of the current $I(t)$ driven in the RCE by the harmonic emf. In the following we keep only components relevant for three-wave coupling (with frequencies $\omega_0+\omega_1=\omega_2$ involved), writing the total current as

$$I(t)=\sum_{k=0}^{2} I^{(k)}(t), \quad I^{(k)}(t)=I_k e^{-i\omega_k t}+\text{c.c.} \tag{2}$$

A nonlinear insertion can be generally described with a voltage-dependent resistance $\mathcal{R}(U)$ and capacitance $\mathcal{C}(U)$. Then the voltage drop on the insertion $U(t)$, caused by $I(t)$, is

$$U(t)=\mathcal{R}(U(t))I(t)+\frac{1}{\mathcal{C}(U(t))}\int_{-\infty}^{t} I(\tau)d\tau. \tag{3}$$

Obviously, even with a harmonic current, this voltage drop is not represented by harmonic oscillations. Therefore, for strong pumping at ω_0 we have to assume in general an arbitrary $2\pi/\omega_0$-periodic time dependence $U^{(0)}(t)$, having a component at ω_0 plus higher harmonics; this dependence can be found for particular insertions as explained below. In contrast, in a linear approximation with respect to weak signal waves, it is sufficient to take into account only the main harmonics of $U(t)$ at ω_1 and ω_2, so that we can summarize the voltage drop, relevant for three-wave coupling, as

$$U(t)=U^{(0)}(t)+\sum_{k=1,2} U^{(k)}(t) \tag{4}$$

$$\text{with } U^{(k)}(t)=U_k e^{-i\omega_k t}+\text{c.c.} \quad \text{only for } k=1,2.$$

Because of nonlinear interaction, the voltages U_k are determined by the currents at all the frequencies involved. In order to determine the coupling strength, we have to express U_k explicitly via these currents. In general, the dependence of $U(t)$ on $I(t)$ is mapped by a functional $U=U[I]$, resulting from the solution of the transcendental equation (3). Whereas no analytical solution can be obtained for that equation in general, under the assumption of strong pumping $I_0 \gg I_{1,2}$ we can perform an expansion with respect to I_1, I_2, keeping only terms linear in I_1, I_2. This results in general coupling equations

$$U_2=I_2X_{22}(I_0)+I_1X_{21}(I_0),$$

$$U_1=I_1X_{11}(I_0)+I_2X_{12}(I_0), \tag{5}$$

where the X factors depend nonlinearly on the pump amplitude; their particular form is determined by the characteristics of the nonlinear insertions $\mathcal{R}(U), \mathcal{C}(U)$, as discussed in detail in the following sections. Provided that we know the X factors, nonlinear coupling between U_1, U_2 and I_1, I_2 is then found.

Next, we return to the response of the whole metamaterial. In accordance with the macroscopic approach (see Ref. [6]), in analyzing the electromagnetic wave interaction with the metastructure we assume that the response is formed at distances much smaller than the wavelength. The corresponding quasistatic limit allows us to separate magnetic and electric effects, so that only the magnetic field affects the magnetization of the metamaterial, which defines the magnetic susceptibility. At this scale, we can also neglect the inhomogeneity of magnetization and averaged fields and the problem is reduced to the behavior of a RCE array in an external homogeneous oscillating magnetic field.

We consider an array of identical RCEs, arranged as a regular three-dimensional (3D) lattice, so that all the elements lie in parallel planes normal to the z axis and all have the same surroundings. Then only the z components of mag-

netic field and the *zz* components of magnetic susceptibility tensor are relevant, and below we omit all appearing *z* and *zz* indices.

Obviously, in a homogeneous medium under the action of an external homogeneous field $\mathcal{H}(\omega)$, all RCEs are in the same situation. Thus the same emf

$$\mathcal{E}(\omega) = i\mu_0 S\omega\mathcal{H}(\omega) \tag{6}$$

is induced in every element, driving the same currents, which, we recall, are assumed to be also harmonic. In Eq. (6), S is the effective area of the RCE contour, which determines the magnetic flux via the element.

Upon taking into account the mutual interaction of the elements, as reported in detail in [6,7], we introduce the total effective impedance $Z_\Sigma(\omega)$. Since the mutual interaction is linear, it affects only the linear properties of RCEs. Then for the frequencies of weak signal waves we can write the extended impedance equations

$$\mathcal{E}_k = Z_\Sigma(\omega_k)I_k + U_k, \quad k = 1,2, \tag{7}$$

where the nonlinear contribution results in additional voltages U_k, given by Eq. (5), and $\mathcal{E}_k$ implies the emf induced solely by the external field at frequency ω_k.

Now, using Eq. (6), we combine the systems (5) and (7), and rewrite them to obtain coupling equations for the magnetization of the metamaterial, $M(\omega_k)$, which is given by the density of the corresponding magnetic moments nSI_k (where n is the volume density of the RCEs):

$$M(\omega_2) = \frac{i\omega_2 nS^2\mathcal{H}(\omega_2) - X_{21}M(\omega_1)}{Z_\Sigma(\omega_2) + X_{22}}. \tag{8}$$

Here and below we write only the ω_2 components for simplicity; expressions for ω_1 are the same except for interchanged indices $1 \leftrightarrow 2$.

We recall that by definition the magnetic induction B is proportional to the spatially averaged microscopic magnetic field: $B = \mu_0\langle H_{\mathrm{mic}}\rangle$. As was shown in [6], corresponding volume integration gives generally $B = \mu_0\left(\mathcal{H} + \frac{2}{3}M\right)$ notwithstanding the structure element's peculiarities. With the general definition $B = \mu_0(H+M)$, we can express the externally applied field $\mathcal{H}$ via the macroscopic magnetic field H inside the medium: $\mathcal{H} = H + \frac{1}{3}M$. Then we finally solve Eq. (8) for M, expressing the magnetization via the macroscopic fields $H(\omega)$ inside the metamaterial in the following form:

$$M(\omega_2) = \chi_{\mathrm{M}}(\omega_2)H(\omega_2) + Y(\omega_2; H_0, \omega_0, \omega_1)H(\omega_1). \tag{9}$$

The linear magnetic susceptibility here is given by

$$\chi_{\mathrm{M}}(\omega_2) = \frac{\mu_0 nS^2\omega_2}{-\frac{1}{3}\mu_0 nS^2\omega_2 - i[Z_\Sigma(\omega_2) + X_{22}(I_0)]}. \tag{10}$$

Note that it is modulated due to the insertion contribution. Thus, the linear properties of the metamaterial at the signal frequencies are dependent on the pump field amplitude. This feature represents a valuable tuning effect, the details of which will be published elsewhere.

The dimensionless factor

$$Y(\omega_2, H_0, \omega_0, \omega_1) = \frac{iX_{21}(I_0)}{\mu_0 nS^2\omega_2}\chi_{\mathrm{M}}(\omega_2)\chi_{\mathrm{M}}(\omega_1) \tag{11}$$

defines the nonlinear modulation of the magnetic susceptibility, and for completeness we have only to express the pump current amplitude I_0 via the pump field amplitude H_0. For strong pumping at one frequency, an additional nonlinear contribution from signal waves to $M(\omega_0)$ and to $\chi_{\mathrm{M}}(\omega_0)$ can be neglected, so that $M(\omega_0) = \chi_{\mathrm{M}}(\omega_0)H(\omega_0)$ and then

$$I_0 = \frac{\chi_{\mathrm{M}}(\omega_0)}{nS}H_0. \tag{12}$$

Equation (11) with relation (12) describe then the strength of nonlinear coupling between the interacting waves.

The expression (9) is analogous to (1), with the notable distinction that the dependence of the nonlinear modulation on H_0 is no longer linear, but is included in the modulation coefficient $Y(\omega_2; H_0, \omega_0, \omega_1)$ via the X_{21} factor. In the limit of weak nonlinearity, the X factors can be easily calculated analytically, leading to linear dependence on H_0 in agreement with Eq. (1), and then Eqs. (10) and (11) coincide with the results reported in Ref. [7].

Considering application capabilities of the metamaterial, it is important to keep in mind that energy dissipation can be essential, especially for insertions with variable resistance. For nonlinear coupling in the form (9), the rate of the energy exchange between the interacting waves depends on the modulation coefficient Y, whereas the wave energy dissipation is determined by the imaginary part of the linear susceptibility. Therefore, in order to enable efficient nonlinear processes, $\mathrm{Im}[\chi_{\mathrm{M}}(\omega)]$ should not exceed Y. Provided that the contribution of insertions is small compared to the linear contour response, we can safely assume that the overall dissipation is small and $\mathrm{Im}[\chi_{\mathrm{M}}(\omega)] \ll \mathrm{Re}[\chi_{\mathrm{M}}(\omega)]$. This entitles us to use the approximation

$$\mathrm{Im}[\chi_{\mathrm{M}}(\omega_2)] \approx |\chi_{\mathrm{M}}(\omega_2)|^2 \frac{\mathrm{Re}[X_{22}]}{\mu_0 nS^2\omega_2}, \tag{13}$$

where we also imply that the resistance R_c of the linear part of the RCE contour is negligible compared to that of the insertion, $\mathrm{Re}[X_{22}]$.

In the following sections we analyze the details of calculating X factors for particular types of insertions and estimate the magnitudes of the nonlinear modulations achievable with use of nonlinear devices reported in the literature.

III. INSERTIONS WITH VARIABLE RESISTANCE

A. Nonlinear modulation

Analyzing the behavior of a diode with variable resistance, inserted into a RCE, we can simplify the general equation (3), which lacks a capacitive term for this case, immediately describing the current-voltage characteristic by an arbitrary function $\mathcal{U}(I)$. This function can be approximated analytically or mapped using direct measurements for a particular insertion. The voltage drop on the insertion is then determined by this function, taken with I given by Eq. (2).

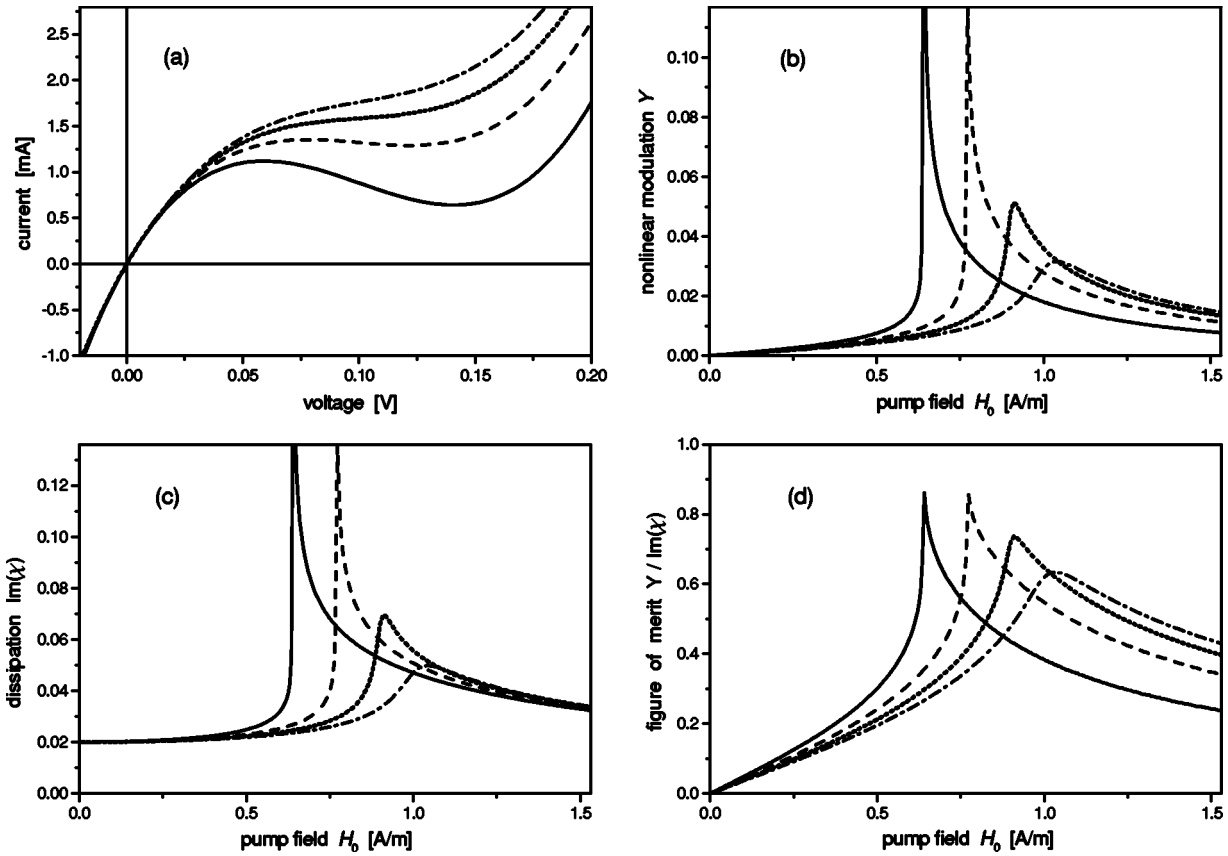

FIG. 1. Backward diodes as nonlinear insertions: (a) model current-voltage characteristics with (solid and dash lines) and without (dot and dash-dot lines) negative resistance range (see the text for details); corresponding dependencies on the pump field amplitude H_0 of (b) nonlinear modulation Y, (c) dissipation $\mathrm{Im}[\chi_M(\omega)]$, and (d) figure of merit $Y/\mathrm{Im}[\chi_M(\omega)]$.

Expanding it up to terms linear with respect to I_1, I_2, we obtain

$$U(t) = \mathcal{U}(I^{(0)}(t)) + \mathcal{U}'(I^{(0)}(t))(I_1 e^{-i\omega_1 t} + I_2 e^{-i\omega_2 t} + \text{c.c.}), \tag{14}$$

where $\mathcal{U}'$ denotes $d\mathcal{U}/dI$. Combining together all the terms with ω_2, we arrive directly at the form (5), e.g.,

$$U_2 = I_2 X_{22}(I_0) + I_1 X_{21}(I_0) \tag{15}$$

where the X factors can be calculated, for a given $\mathcal{U}(I)$ dependence, as the zero and first Fourier coefficients of the $\mathcal{U}'$ $(I^{(0)}(t))$ function:

$$X_{22}(I_0) = \frac{\omega_0}{2\pi}\int_0^{2\pi/\omega_0} \mathcal{U}'(I^{(0)}(t))dt, \tag{16}$$

$$X_{21}(I_0) = \frac{\omega_0}{2\pi}\int_0^{2\pi/\omega_0} \mathcal{U}'(I^{(0)}(t))e^{-i\omega_0 t}dt. \tag{17}$$

Then the nonlinear modulation (11) and dissipation (13) can be obtained for particular insertion characteristics and metamaterial parameters.

B. Practical estimates for backward diodes

To make use of variable resistance, we suggest employing backward diodes. They are notable for high sensitivity, which would enable relatively low pump amplitudes, and are commonly used in the operational range around zero voltage, requiring no additional bias.

The characteristics of particular backward diodes may vary essentially, but here we would like to give merely qualitative estimates. To choose some particular parameters we refer to a typical set of InGaAs diodes, reported to be designed for high nonlinearity [20]. The current-voltage characteristics demonstrated there have a different appearance, but what is essential for nonlinear effects is the curvature of the current-voltage dependence, while the scaling along either axis *per se* is not relevant for comparative analysis.

Accordingly, we model a set of current-voltage characteristics by functions $\mathcal{J}(U)$, which show qualitative agreement with the experimental curves [20] within the intended operating range [Fig. 1(a)]. All the functions have the same initial slope, corresponding to 10 Ω zero-bias resistance (which implies $10^{-2}-10^{-3}$ mm^2 diode cross section).

To calculate the X factors, we imply, in accordance with the above assumptions, that the diode in the RCE is forced to an external harmonic pump current $I^{(0)}(t)$, and for this current we obtain $U(t)$ by solving $\mathcal{J}(U(t)) = I^{(0)}(t)$ numerically.

To estimate the resulting nonlinear modulation (11), we take the example of a metamaterial similar to that of Ref. [6], with circular RCEs with 5 mm radius and 1 mm wire diameter, arranged in parallel planes with tetragonal symmetry with 2.2 radii in-layer spacing and half radius interlayer

spacing. Such RCE dimensions provide self-inductance of about 12 nH; choosing a contour capacitance about 0.02 pF we arrive at the single element resonance frequency of $2\pi \times 10^{10}$ rad/s. With the above lattice constants, the resonance frequency of the effective magnetic susceptibility occurs at $1.2\pi \times 10^{10}$ rad/s. We assume that the metamaterial is employed below resonance, so that $\chi_M(\omega_1), \chi_M(\omega_2)$ are of the order of unity. This corresponds to wavelengths of the order of 10 cm, quite acceptable for the chosen RCE size.

In Fig. 1(b) we plot the nonlinear modulation $|Y(\omega_2, H_0, \omega_0, \omega_1)|$ as a function of pump field amplitude H_0, for each of the modeled current-voltage characteristics shown in Fig. 1(a). It is remarkable that these dependencies have a qualitatively different appearance: for the characteristics having a "negative resistance" range [Fig. 1(a), solid and dash lines] sharp pronounced maxima are obtained, while for those that are monotonic [Fig. 1(a), dot and dash-dot lines] the maxima are smooth.

Such behavior is expected from the expression (17) for the X_{21} factor, responsible for nonlinearity. Indeed, this factor is determined by the integration over $\mathcal{U}'(I)$ values. The current-voltage characteristics of the first type have points I_∞ where $\mathcal{U}'(I)$ tends to infinity. They correspond to unstable states of the diode, so when the current amplitude is larger than I_∞, they are rapidly crossed by $I(t)$ in a hysteresislike way, and do not contribute much to the integral. However, the closer is the amplitude to I_∞, the more time the diode spends in the state with high $\mathcal{U}'(I)$ values [because the oscillating $I(t)$ is around the turning point there]. In an ideal case, when I_0 matches I_∞ exactly, X_{21} would tend to infinity, and so would the nonlinear modulation. Obviously, this condition cannot be reached in reality due to unavoidable inhomogeneity of the diodes, RCEs, their arrangement, etc., otherwise negligible. Moreover, significant increase in the effective diode resistance for signal waves would make the approach presented here inappropriate, as the requirement of weak insertion contribution would not hold. In principle, this situation could give rise to numerous interesting effects, investigation of which is, however, beyond the aim of this paper. Supposing that all the limitations would not allow extremely high X factors, we still expect that nonlinearity observed in real systems will be rather sensitive to the pump amplitude in the narrow range around I_∞.

In contrast, for monotonic characteristics no such peculiarities are expected, and smooth maxima are reached when the current amplitudes are in the range where $\mathcal{U}'(I)$ has maximal values.

As seen from Fig. 1(b), an exceptionally high nonlinear modulation, about 0.05 and more, can be achieved with moderate pump fields, about 1 A/m.

Note that the X_{22} factor (16), responsible for dissipation in the metamaterial, also involves integration over $\mathcal{U}'(I)$. Therefore, $\mathrm{Im}[\chi_M(\omega)]$ (13) shows similar behavior with respect to pump amplitudes [Fig. 1(c)]. In the limit of zero pumping, it is determined by the zero-bias resistance, as expected.

The results in Fig. 1(b) and Fig. 1(c) show that both nonlinearity modulation Y and dissipation, characterized by $\mathrm{Im}[\chi_M(\omega)]$, not only have qualitatively similar dependence on I_0, but also reach comparable magnitudes. In Fig. 1(d) we plot the ratios $|Y(\omega_2, H_0, \omega_0, \omega_1)|/\mathrm{Im}[\chi_M(\omega_2)]$. These ratios appear to be below unity for all the current-voltage characteristics; this is not surprising in view of the resistive nature of the nonlinearity. This feature might limit the application of backward diodes in metamaterials designed for nonlinear processes concerned with wave coupling. On the other hand, it is quite useful for other applications like tunable metamaterials, analysis of which will be published elsewhere.

Insertions with variable capacitance, which are discussed below, possess a different nonlinearity origin and are, therefore, free from this limitation.

IV. INSERTIONS WITH VARIABLE CAPACITANCE

A. Nonlinear modulation

We assume such an insertion to possess a voltage-dependent capacitance $\mathcal{C}(U)$ and constant resistive losses $\mathcal{R}$. Although the latter holds only for particular varactors [22], as long as the quality factor is high at the frequencies concerned, $\mathcal{R} \ll |1/(\omega\mathcal{C})|$, the resistance does not provide a remarkable contribution to the nonlinear modulation. Thus, we neglect the $\mathcal{R}(U)$ dependence in Eq. (3) for simplicity. Then the voltage drop at the insertion obeys the equation

$$U(t) = \mathcal{R}I(t) + \frac{1}{\mathcal{C}(U(t))}\int_{-\infty}^{t} I(\tau)d\tau, \tag{18}$$

and we have to analyze it with current (2) and voltage (4). We recall that the pumping is expected to be only slightly distorted by the insertion, so that $I^{(0)}(t) \gg I^{(1,2)}(t)$ and $U^{(0)}(t) \gg U^{(1,2)}(t)$. Therefore, in order to determine the voltage drop caused by pumping we take into account only $U^{(0)}(t)$ and the harmonic $I^{(0)}(t)$ in Eq. (18). Then we arrive at a transcendental equation

$$U^{(0)}(t) = \mathcal{R}(I_0 e^{-i\omega_0 t} + \text{c.c.}) + \frac{1}{\mathcal{C}(U^{(0)}(t))}\left(\frac{I_0 e^{-i\omega_0 t}}{-i\omega_0} + \text{c.c.}\right), \tag{19}$$

which can be solved numerically for a given $\mathcal{C}(U)$ dependence. In general, this results in $U^{(0)}(t)$ having components at ω_0 and its multiples.

Next, considering Eq. (18) for signal components, in the linear approximation we can perform an expansion

$$\frac{1}{\mathcal{C}(U(t))} \approx \frac{1}{\mathcal{C}(U^{(0)}(t))} + \left(\frac{1}{\mathcal{C}(U^{(0)}(t))}\right)' \times (U_1 e^{-i\omega_1 t} + U_2 e^{-i\omega_2 t} + \text{c.c.}), \tag{20}$$

where we denote

$$\left(\frac{1}{\mathcal{C}(U^{(0)}(t))}\right)' \equiv \left|\frac{d}{dU}\left(\frac{1}{\mathcal{C}(U)}\right)\right|_{U=U^{(0)}(t)}.$$

For a known $U^{(0)}(t)$ function, both fractions in Eq. (20) can be written as the corresponding Fourier expansions

$$\frac{1}{\mathcal{C}(U^{(0)}(t))} = \sum_{n=0}^{\infty} K_n e^{-in\omega_0 t} + \text{c.c.},$$

$$\left(\frac{1}{\mathcal{C}(U^{(0)}(t))}\right)' = \sum_{n=0}^{\infty} G_n e^{-in\omega_0 t} + \text{c.c.}, \tag{21}$$

with Fourier coefficients

$$K_n = \frac{\omega_0}{2\pi}\int_0^{2\pi/\omega_0} \frac{1}{\mathcal{C}(U^{(0)}(t))} e^{-in\omega_0 t} dt,$$

$$G_n = \frac{\omega_0}{2\pi}\int_0^{2\pi/\omega_0} \left(\frac{1}{\mathcal{C}(U^{(0)}(t))}\right)' e^{-in\omega_0 t} dt. \tag{22}$$

Now we can insert the obtained expansions (21) into Eq. (18), and combine the terms contributing at ω_1 and ω_2, taking $\omega_0+\omega_1=\omega_2$ into account. Keeping only the terms linear with respect to I_1, I_2, U_1, U_2 provides us with a linear system of equations, which is omitted here owing to its cumbersome appearance; it can be solved straightforwardly, enabling us to express U_2 via I_1 and I_2 in the form (5), with the X factors given, upon algebraic simplification, by

$$X_{21} = \frac{\omega_0}{\omega_1}\frac{G_0 I_0(K_0 - i\omega_1\mathcal{R}) - K_1(i\omega_0 - G_1 I_0^* + G_1^* I_0)}{(i\omega_0 - G_1 I_0^* + G_1^* I_0)^2 + G_0^2 I_0 I_0^*}, \tag{23}$$

$$X_{22} = \frac{\omega_0}{\omega_2}\frac{G_0 I_0 K_1 - (K_0 - i\omega_2\mathcal{R})(i\omega_0 - G_1 I_0^* + G_1^* I_0)}{(i\omega_0 - G_1 I_0^* + G_1^* I_0)^2 + G_0^2 I_0 I_0^*}. \tag{24}$$

Then the nonlinear modulation (11) and dissipation (13) can be calculated for particular metamaterial parameters.

B. Practical estimates for varactors

Obviously, varactors appropriate for practical realization of the three-wave coupling have to possess a nonsymmetric capacitance-voltage characteristic. An overview of recent publications [21–24] allows us to infer that such devices are available for application in the gigahertz range with good enough quality factors. Without going into details of particular data, in the illustrative estimates below we rely on typical parameters [22] and model capacitance-voltage characteristics by a set of algebraic $\mathcal{C}(U)$ functions [Fig. 2(a)]. We assign the same zero-bias capacitance $C_0=0.2$ pF (so that $C_0 \gg C_c$) and the same sensitivity to voltage to all the functions, as changing these parameters results only in scaling without qualitative difference in the nonlinear response we are looking for. Instead, we have chosen to vary the ratio of the capacitance C_1, observed at a certain large voltage, to C_0.

In Fig. 2(b) we plot the nonlinear modulation as a function of pump field amplitude, calculated for each of the modeled functions. It shows significant increase as the pump amplitude exceeds a certain value. It is notable that the sensitivity of nonlinear modulation to the pumping depends remarkably on the C_1/C_0 ratio, with $Y(H_0)$ being much steeper for a merely 2-3 times lower ratio. With the accepted practical parameters (see Sec. III B) we estimate that enormous nonlinear modulation of the order of 0.1 is achievable with quite feasible field amplitudes, about 0.2–0.5 A/m.

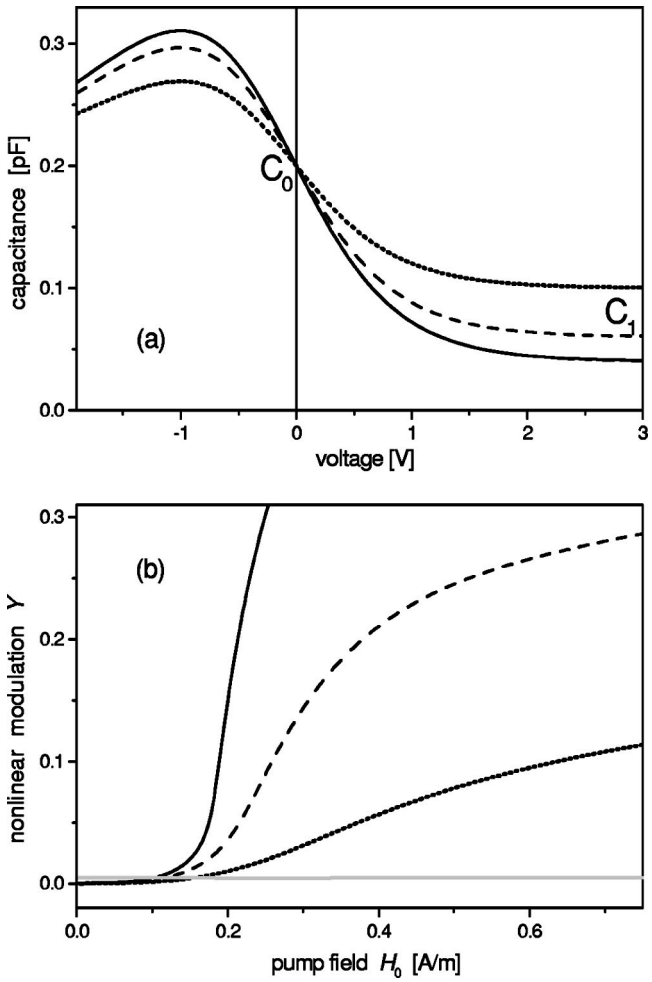

FIG. 2. Varactor diodes as nonlinear insertions: (a) model capacitance-voltage characteristics with C_1/C_0 ratios 0.2 (solid), 0.3 (dash), 0.5 (dot); (b) corresponding nonlinear modulation $Y(H_0)$ and dissipation $\mathrm{Im}[\chi_M(\omega)]$ (gray line).

The data in Fig. 2 suggest even higher modulation, but this is not acceptable within the frame of approach presented here. Already a 10% modulation is incomparably higher than the magnitudes known in optics. This implies that such a metamaterial can be effective with by far less optimal parameters than those taken for estimates here.

For comparison, we also plot $\mathrm{Im}[\chi_M(\omega)]$, assuming the quality factor of the varactor itself to be about 100 [Fig. 2(b), gray line]. We see that dissipation does not depend markedly on the pumping, which is not surprising when the $\mathcal{R}(I)$ dependence is negligible. This means, in particular, that with poorer quality factors nonlinear modulation that exceeds losses still can be obtained, though with more intense pumping.

Despite these promising estimates, varactor diodes have some disadvantages; namely, they experience avalanche breakdown at moderate voltage, and they often have subdued performance at high frequencies. This limits either the suitable field amplitudes and therefore, achievable nonlinearity, or the range of operating frequencies.

The abovementioned disadvantages of varactors are overcome in variable capacitance devices based on ferroelectric

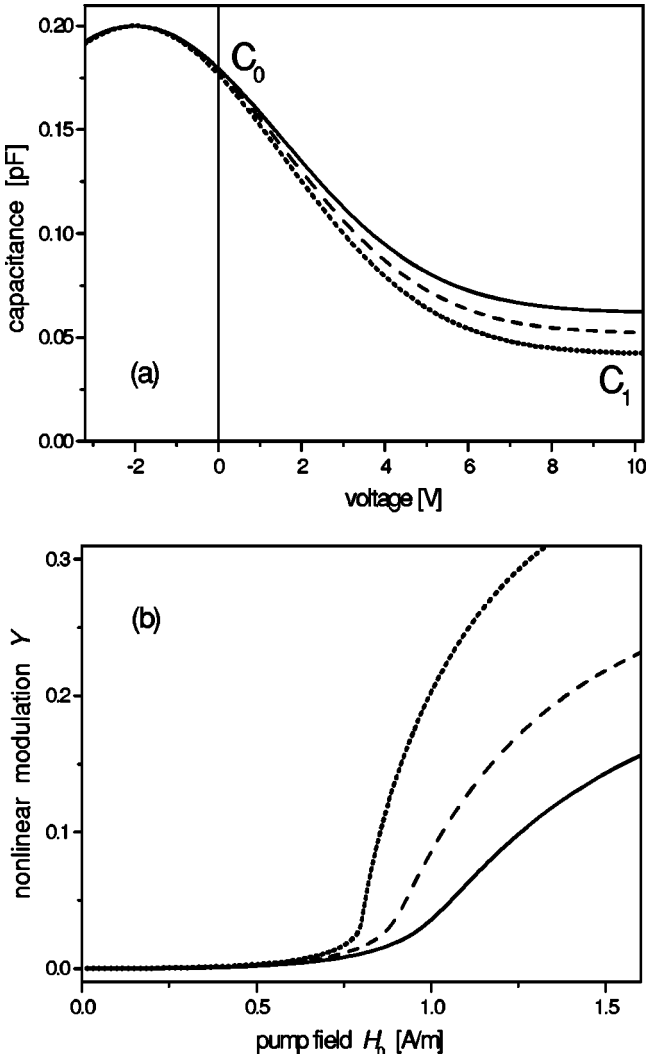

FIG. 3. Biased ferroelectric films as nonlinear insertions: (a) model capacitance-voltage characteristics, with C_1/C_0 ratios 0.2 (solid), 0.25 (dash), 0.3 (dot); (b) corresponding nonlinear modulation $Y(H_0)$.

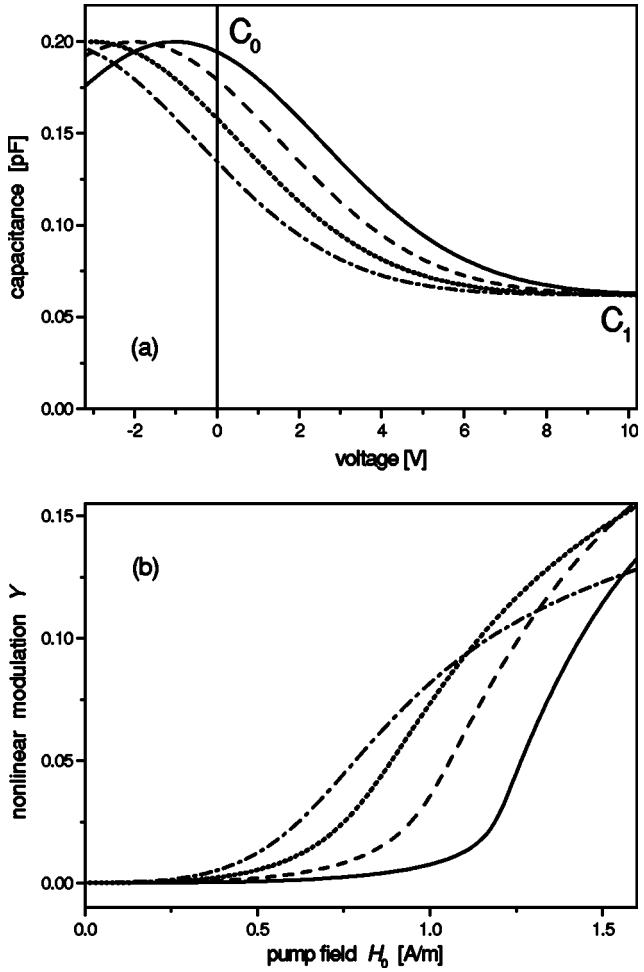

FIG. 4. Controlling nonlinearity by bias: (a) model capacitance-voltage characteristics ($C_1/C_0=0.3$); (b) corresponding nonlinear modulation $Y(H_0)$. Ferroelectric films are biased by 1 V (solid), 2 V (dash), 3 V (dot), 4 V (dash-dot).

films [25,26]. These can tolerate much higher voltages and can be employed at frequencies up to the terahertz range, which are even higher than presently intended for metamaterials. However, varactors based on ferroelectric films possess symmetric capacitance-voltage characteristics, and therefore require an additional bias in order to be employed in three-wave coupling processes.

A way conventional in electronics to bias a diode by means of an external voltage supply might be acceptable for a single RCE or a planar configuration [27], but is hardly ever realizable in 3D metamaterials. We propose, instead, to bias the diode with a voltage drop caused by an emf, induced in the RCE by an additional external magnetic field $H_b(t)$, varying at times much larger than the period of the interacting signals.

From typical data [26], used for estimates below, we presume that the required bias voltage U_b is of the order of volts. To estimate the corresponding external biasing field we note that for a slowly varying field, the induced emf $\mathcal{E}_b(t)=-\mu_0 S\dot{H}_b(t)$ entirely results in voltage drops on the capacitances C_c of the RCE contour and $\mathcal{C}(U_b)$ of the diode. Then the voltage on the diode is given by

$$U_b = -\frac{C_c}{\mathcal{C}(U_b)+C_c}\mu_0 S\dot{H}_b,$$

from which characteristic $\dot{H}_b$ amplitudes are obtained. With $\mathcal{C}(U_b)/C_c \sim 10$ we arrive at $\dot{H}_b \sim 10^{-11}$ A/(m s), which means, for instance, fields about 1000 A/m varying at a characteristic time about 10 ns.

For a qualitative illustration, we model $\mathcal{C}(U)$ dependencies, similar to those in Ref. [26], with simple functions, shifted (biased) from symmetrical with respect to the $U=0$ position. The maximal capacitance C_0 is kept the same for all the functions, while either the "minimal" capacitance C_1 [Fig. 3(a)] or bias [Fig. 4(a)], is the variable parameter. The corresponding dependencies of the nonlinear modulation on the pump field intensity, calculated for these sets of functions, are plotted in Fig. 3(b) and Fig. 4(b), respectively. We do not plot $\mathrm{Im}[\chi_M(\omega)]$ there, as it demonstrates similar behavior as in Fig. 2, being much smaller than the achievable nonlinearity.

Figure 3(b) shows that the nonlinear modulation grows essentially with increasing pump amplitude above a certain value, which is independent of the C_1/C_0 ratio, while the rate of nonlinearity growth is remarkably sensitive to this ratio. This behavior is analogous to what occurs for nonsymmetric varactor diodes; it is not surprising, as the model $\mathcal{C}(U)$ functions are qualitatively similar in these two cases. The exceptional modulation of the order of 0.1 is reached here at larger pump amplitudes, in accordance with higher operating voltages for devices based on ferroelectric films.

Increasing bias, as shown in Fig. 4(b), results in lower pump fields required to achieve essential nonlinearity. This enables controlling the strength of nonlinear coupling: varying the biasing field with a fixed pump intensity leads to significant change in the nonlinear modulation. Such tuning of the nonlinear response has no direct analogy in optical crystals and represents an example of the advantageous controllability of the metamaterial.

V. DISCUSSION

In summary, we developed an approach for calculating the nonlinear modulation of magnetic susceptibility in a metamaterial with insertions operating in an essentially nonlinear regime. We have shown that the dependence of the modulation on the pump field amplitude is remarkably nonlinear, with the peculiarities determined by the type of insertion and its particular characteristics.

Practical estimates, relying on the diodes' characteristics reported in the current literature, predict that exceptionally high nonlinear modulation of magnetic susceptibility, up to 0.1, can be achieved. Such an enormous value exceeds by many orders of magnitude nonlinearities known in optics. Note that in the illustrative examples we neither claim to have chosen optimal insertion properties, nor intend to suggest necessarily the particular diodes, mentioned above, for practice. We rather propose a universal method for deriving metamaterial properties from the known characteristics of insertions, whichever appear appropriate for experiment. General recommendations for choosing them, however, can be acquired already from the illustrations here.

We point out a valuable advantage that in the considered metamaterial the nonlinear response can be tuned by applying an external varying magnetic field. This feature, having no direct analogy in optics, can offer additional improvements to conventional nonlinear applications as well as new unusual techniques.

We believe that the approach developed here represents the basis for analysis of metamaterials with nonlinear insertions, and that it can be further extended in order to describe other kinds of nonlinear processes.

ACKNOWLEDGMENT

Financial support from the Deutsche Forschungsgemeinschaft is gratefully acknowledged by M.L. (Graduate College 695).

[1] V. G. Veselago, Usp. Fiz. Nauk **92**, 517 (1967) [Sov. Phys. Usp. **10**, 509 (1968)].
[2] J. B. Pendry, A. J. Holden, D. J. Robbins, and W. J. Stewart, IEEE Trans. Microwave Theory Tech. **47**, 2075 (1999).
[3] R. A. Shelby, D. R. Smith, and S. Schultz, Science **292**, 77 (2001).
[4] M. Bayindir, K. Aydin, E. Ozbay, P. Markoš, and C. M. Soukoulis, Appl. Phys. Lett. **81**, 120 (2002).
[5] I. V. Lindell, S. A. Tretyakov, K. I. Nikoskinen, and S. Ilvonen, Microwave Opt. Technol. Lett. **31**, 129 (2001).
[6] M. Gorkunov, M. Lapine, E. Shamonina, and K. H. Ringhofer, Eur. Phys. J. B **28**, 263 (2002).
[7] M. Lapine, M. Gorkunov, and K. H. Ringhofer, Phys. Rev. E **67**, 065601 (2003).
[8] J. D. Jackson, *Classical Electrodynamics* (Willey, New York, 1999).
[9] L. D. Landau and E. M. Lifschitz, *Electrodynamics of Continuous Media* (Pergamon Press, Oxford, 1984).
[10] M. V. Gorkunov and M. I. Ryazanov, JETP **85**, 97 (1997).
[11] V. A. Kalinin and V. V. Shtykov, Sov. J. Commun. Technol. Electron. **36**, 96 (1991).
[12] S. A. Tretyakov, Microwave Opt. Technol. Lett. **31**, 163 (2001).
[13] A. A. Zharov, I. V. Shadrivov, and Y. S. Kivshar, Phys. Rev. Lett. **91**, 037401 (2003).
[14] V. M. Agranovich, Y. R. Shen, R. H. Baughman, and A. A. Zakhidov, Phys. Rev. B **69**, 165112 (2004).
[15] S. O'Brien, D. McPeake, S. A. Ramakrishna, and J. B. Pendry, Phys. Rev. B **69**, 241101(R) (2004).
[16] D. R. Smith, W. J. Padilla, D. C. Vier, S. C. Nemat-Nasser, and S. Schultz, Phys. Rev. Lett. **84**, 4184 (2000).
[17] R. A. Shelby, D. R. Smith, S. C. Nemat-Nasser, and S. Schultz, Appl. Phys. Lett. **78**, 489 (2001).
[18] M. Shamonin, E. Shamonina, V. Kalinin, and L. Solymar, J. Phys. D **37**, 362 (2004).
[19] R. Marqués, F. Medina, and R. Rafii-El-Idrissi, Phys. Rev. B **65**, 144440 (2002).
[20] J. N. Schulman, D. H. Chow, and D. M. Jang, IEEE Electron Device Lett. **22**, 200 (2001).
[21] O. Vanbésien, G. Beaudin, and J. C. Pernot, J. Phys. IV **9**, 151 (1999).
[22] M. Mamor *et al.*, Appl. Phys. A: Mater. Sci. Process. **72**, 633 (2001).
[23] M. Marso *et al.*, Electron. Lett. **37**, 1476 (2001).
[24] S. Abadei, S. Gevorgian, C.-R. Cho, and A. Grishin, J. Appl. Phys. **91**, 2267 (2002).
[25] A. Kozyrev *et al.*, J. Appl. Phys. **88**, 5334 (2000).
[26] R. A. York *et al.*, Integr. Ferroelectr. **34**, 177 (2001).
[27] O. Reynet and O. Acher, Appl. Phys. Lett. **84**, 1198 (2004).